HAL
archives-ouvertes.fr

# Combination of Polyaffine Transformations and Supervised Learning for the Automatic Diagnosis of LV Infarct

Marc-Michel Rohé, Nicolas Duchateau, Maxime Sermesant, Xavier Pennec

▶ **To cite this version:**

Marc-Michel Rohé, Nicolas Duchateau, Maxime Sermesant, Xavier Pennec. Combination of Polyaffine Transformations and Supervised Learning for the Automatic Diagnosis of LV Infarct. Statistical Atlases and Computational Models of the Heart. Imaging and Modelling Challenges. STACOM 2015., 2015, Munich, Germany. pp.190-198. hal-01206710

**HAL Id: hal-01206710**
**https://hal.inria.fr/hal-01206710**

Submitted on 29 Sep 2015

**HAL** is a multi-disciplinary open access archive for the deposit and dissemination of scientific research documents, whether they are published or not. The documents may come from teaching and research institutions in France or abroad, or from public or private research centers.

L'archive ouverte pluridisciplinaire **HAL**, est destinée au dépôt et à la diffusion de documents scientifiques de niveau recherche, publiés ou non, émanant des établissements d'enseignement et de recherche français ou étrangers, des laboratoires publics ou privés.

# Combination of Polyaffine Transformations and Supervised Learning for the Automatic Diagnosis of LV Infarct

Marc-Michel Rohé, Nicolas Duchateau, Maxime Sermesant and Xavier Pennec

Inria Sophia-Antipolis, Asclepios Research Group, Sophia-Antipolis, France

**Abstract.** In this article, we present an application of the polyaffine transformations to classify a population of hearts with myocardial infarction. Polyaffine transformations aim at representing motion by the combination of a limited number of affine transformations defined locally on a regional division of the space. We show that these transformations not only serve as a first (non-learnt) dimension reduction, but also allow to interpret each of the parameters and relate them to known clinical parameters. Then, we use standard supervised learning algorithms on these parameters to classify the population between infarcted and non-infarcted subjects. The method is applied on the STACOM statistical shape modeling labeled data consisting of 200 cases, comprising the same number of healthy subjects and patients with infarct. We train classifiers using different standard machine learning algorithms. Finally, we validate our method with 10-fold cross-validation and get more than 95 % of correct classification on yet-unseen data. The method is promising and ready to be tested on the remaining 200 test cases of the challenge.

## 1 Introduction

Myocardial infarction occurs when blood flow to the heart muscle is lowered and the myocardial cells in the territory start dying. The local contractility is reduced and can lead, if prolonged, to severe remodelling of the heart to maintain physiological constraints [1]. The function of the heart is then impaired [2], and is no longer able to pump as efficiently as it used to, which might cause complications. Acute complications may include heart failure if the damaged heart is no longer able to pump blood adequately around the body. Therefore, a quantitative understanding of this pathology and how the heart function changes with an infarct is highly desired. Several methods for computer-aided diagnosis of infarct have already been developed using echocardiographic images of the heart coupled with pattern recognition algorithms [3] although none of the features used are explicitly related to physiological characteristics of cardiac function.

In this article, our goal is to classify between control subjects and patients with infarct in an automatic way, based on the STACOM statistical shape modeling labeled data [4] which consist of a segmentation of the myocardium (both epi and endo) wall at end-diastole and at end-systole. These two categories of

subjects may differ both in the shape of the heart and in the deformation along the cycle. Indeed, after an infarct the damaged region will tend to shrink and the deformation along the cycle will be lower. Similar studies have already been done with the same dataset as [5], which focuses on the shape differences between both population whereas we use both shape and motion features. Due to the complexity and high-dimensionality of these data, we try to quantify both shape and motion using a limited number of parameters, which we combine and use to compare patients and learn the main modes characterizing both populations.

The features of interest characterizing the shape of the patients consist of the regional thickness at both end-diastole and end-systole. We also use features representing the deformation along the cycle. Our approach relies on statistics on the motion of the heart between end-diastole and end-systole. We project the motion on the subspace of polyaffine transformations [6]. With these transformations, we can express a deformation with a limited number of parameters [7]. We develop further the methodology by reducing the transformations to keep only the most relevant parameters.

Then, we test classical machine learning algorithms on our set of combined shape/motion parameters and compare the performance of each algorithm using cross-validation techniques. Validating the method with 10-fold cross-validation, we get results of 95% correct labeling on yet-unseen cases. In addition, our method notably highlights the relative importance of the different features for the classification of this population.

## 2 Extraction of features of interest through shape and motion dimensionality reduction

In this section, we introduce the first dimensionality reduction that is applied to the studied data (made of one segmentation at end-diastole and one at end-systole, each comprised of 1089 points both for the endocardium and the epicardium). It consists in a non-learning approach to project the data of these segmentations to a limited number of regional parameters representing motion and shape.

### 2.1 Polyaffine projection

Due to point to point correspondence of the meshes and prior registration, we already have an estimate of the displacement field $\phi$ mapping each point at end-diastole to the corresponding point at end-systole. Instead of looking at displacements fields, we choose to represent the cardiac motion by the stationary velocity fields (SVF) $\mathbf{v}$ such that $\mathbf{v} = \log \phi$. Working with SVF allows to perform vectorial statistics on diffeomorphisms, while preserving the invertibility constraint, contrary to the Euclidian statistics on displacement fields.

In [6], the authors introduce the space of Log-Euclidean Polyaffine Transformations (LEPT). By defining $K$ regions and smooth weights $\omega_k(x)$, these

transformations have the properties to describe locally affine deformations using few parameters while still being invertible. The polyaffine transformation is the weighted sum of these locally-affine transformations $\mathbf{M}_k$:

$$\mathbf{v}_{poly}(x) = \sum_{k=1}^{K} \omega_k(x) \mathbf{M}_k \tilde{x}.$$

In the case of cardiac motion, we have a standardized regional decomposition into the standard American Heart Association (AHA) 17 regions for the left ventricle. We define the weights $\omega_k$ as normalized Gaussian functions around the barycenter $\bar{x}_k$ of each region such that:

$$\tilde{\omega}_k(x) = \exp\left(\frac{\kappa}{2}(x-\bar{x}_k)^T \phi_k^{-1}(x-\bar{x}_k)\right), \quad \omega_k(x) = \frac{\tilde{\omega}_k(x)}{\sum_{j=1}^{N} \tilde{\omega}_j(x)}.$$

If we gather the parameters of the polyaffine transformation into a large vector $m$ such that $\mathbf{m} = \text{vect}(\mathbf{M}_1, ..., \mathbf{M}_K)$. The parameters of the optimal projection of a Stationary Velocity Fields $\mathbf{v}$ onto the space of polyaffine transformations has an analytical solution [7] $\mathbf{m} = \hat{\mathbf{m}} = \mathbf{\Sigma}^{-1} b$, which minimizes in the least-squares sense:

$$C(\mathbf{M}_1, ..., \mathbf{M}_K) = \int_\Omega \|v_{poly}(x) - v(x)\|^2 dx \simeq \tfrac{1}{2}(\mathbf{m}-\hat{\mathbf{m}})^T \mathbf{\Sigma}(\mathbf{m}-\hat{\mathbf{m}}) - \tfrac{1}{2}\hat{\mathbf{m}}\mathbf{\Sigma}\hat{\mathbf{m}}.$$

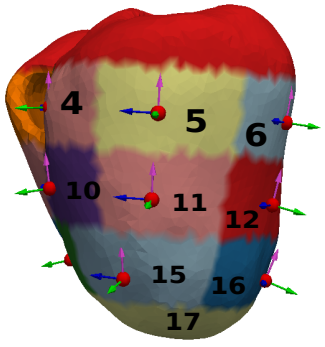


In order to get interpretable parameters for each region, we choose to express them in a local coordinate system adapted to the geometry of the heart. If we call $\mathcal{R} = (\mathbf{O}, \mathbf{e}_1, \mathbf{e}_2, \mathbf{e}_3)$ the original Cartesian coordinate system, we define the local coordinate of the region $k$ as $\mathcal{R}'_i = (\mathbf{O}_k, \mathbf{e}_1^k, \mathbf{e}_2^k, \mathbf{e}_3^k)$ where $\mathbf{O}_k$ is the barycenter of the region (the red point in the enclosed figure), $\mathbf{e}_1$ the radial vector (green vector), $\mathbf{e}_2$ the longitudinal vector (purple vector) and $\mathbf{e}_3$ the circumferential vector (blue vector). We can express the polyaffine parameters $\mathbf{M} = (\mathbf{R}, \mathbf{T})$, where $\mathbf{R}$ is the $3 \times 3$ matrix of the rotational parameters and $\mathbf{T}$ is the translation, in this new frame through the equations:

$$\begin{aligned} \mathbf{R}'_k &= \mathbf{P}_k^{-1} \mathbf{R}_k \mathbf{P}_k \\ \mathbf{T}'_k &= \mathbf{P}_k^{-1}(\mathbf{R}_k \mathbf{O}_k + \mathbf{T}_k), \end{aligned}$$

where $\mathbf{P}_k$ is the transfer matrix from the base $(\mathbf{e}_1, \mathbf{e}_2, \mathbf{e}_3)$ to the base $(\mathbf{e}_1^k, \mathbf{e}_2^k, \mathbf{e}_3^k)$. Then, the new expression of the parameters in this local coordinates system:

$$\mathbf{M}' = \begin{bmatrix} s_r & a_{1,2} & a_{1,3} & t_r \\ a_{2,1} & s_l & a_{2,3} & t_l \\ a_{3,1} & a_{3,2} & s_c & t_c \end{bmatrix},$$

can be related to physiological deformation. The 3 translation parameters correspond to the motion along the 3 local axes (radial, longitudinal, and circumferential) whereas the diagonal coefficients correspond to the strain along these directions.

We propose a method to further reduce the model by keeping only the 3 parameters of the motion and the 3 parameters of the strain. This defines a polyaffine projection that, when expressed in the local basis previously defined, has only these parameters not equal to zero. We first introduce the projection matrix $\mathbf{Q}$ which is a $12K \times 6K$ matrix giving the relation between the $6K$ translation and diagonal parameters expressed in the local coordinates $\mathbf{m_L}$ and the $12K$ parameters expressed in the original coordinates $\mathbf{m}$, such that $\mathbf{Q}\mathbf{m_L} = \mathbf{m}$. When expressing $\mathbf{m}$ this way, we constrain it to be within the subspace spanned by $\mathbf{Q}$. This subspace corresponds exactly to the polyaffine transformation whose non-diagonal and non-translation parameters are equal to zero in the local coordinates. The least-square minimization can now be rewritten as:

$$C(\mathbf{m}) \simeq \frac{1}{2}(\mathbf{Q}\mathbf{m_L} - \hat{\mathbf{m}})^T \mathbf{\Sigma} (\mathbf{Q}\mathbf{m_L} - \hat{\mathbf{m}}) - \frac{1}{2}\hat{\mathbf{m}}\mathbf{\Sigma}\hat{\mathbf{m}}$$

$$\frac{\partial C}{\partial \mathbf{m_L}} = \mathbf{Q}^T \mathbf{\Sigma}(\mathbf{Q}\mathbf{m_L} - \hat{\mathbf{m}}) = 0 \quad \Longrightarrow \mathbf{m} = \mathbf{Q}\mathbf{m_L} = \mathbf{Q}(\mathbf{Q}^T\mathbf{\Sigma}\mathbf{Q})^{-1}\mathbf{Q}^T \Sigma \hat{\mathbf{m}}$$

For each of the 200 training data we compute the LEPT projection of the deformation field. We are able to parametrize the 3D displacement fields (made of 6534 parameters: 3 parameters for each of the 2178 points of the mesh) by only $6K = 102$ polyaffine parameters. Despite this large reduction of dimensionality, these parameters explain on average more than 70% of the original displacement. Box-plots of each of the 6 parameters are shown in Figure 1, where the most discriminant parameters ($p$ value $< 0.001$) are highlighted in bold. The radial displacement as well as the strain are significantly lower (in absolute value) for the infarcted subjects, which is consistent with what would be clinically expected. Similar differences can be seen for the longitudinal parameters. On the other side, the circumferential motion is less significant, mostly due to the fact that it is very hard to track it accurately with clinical images and therefore not reflected in the provided meshes.

### 2.2 Thickness parameters

On top of the polyaffine parameters that characterize the deformation of the heart during a cardiac cycle, we also introduce parameters representing the overall shape of the heart. We choose to study the thickness of the wall within each of

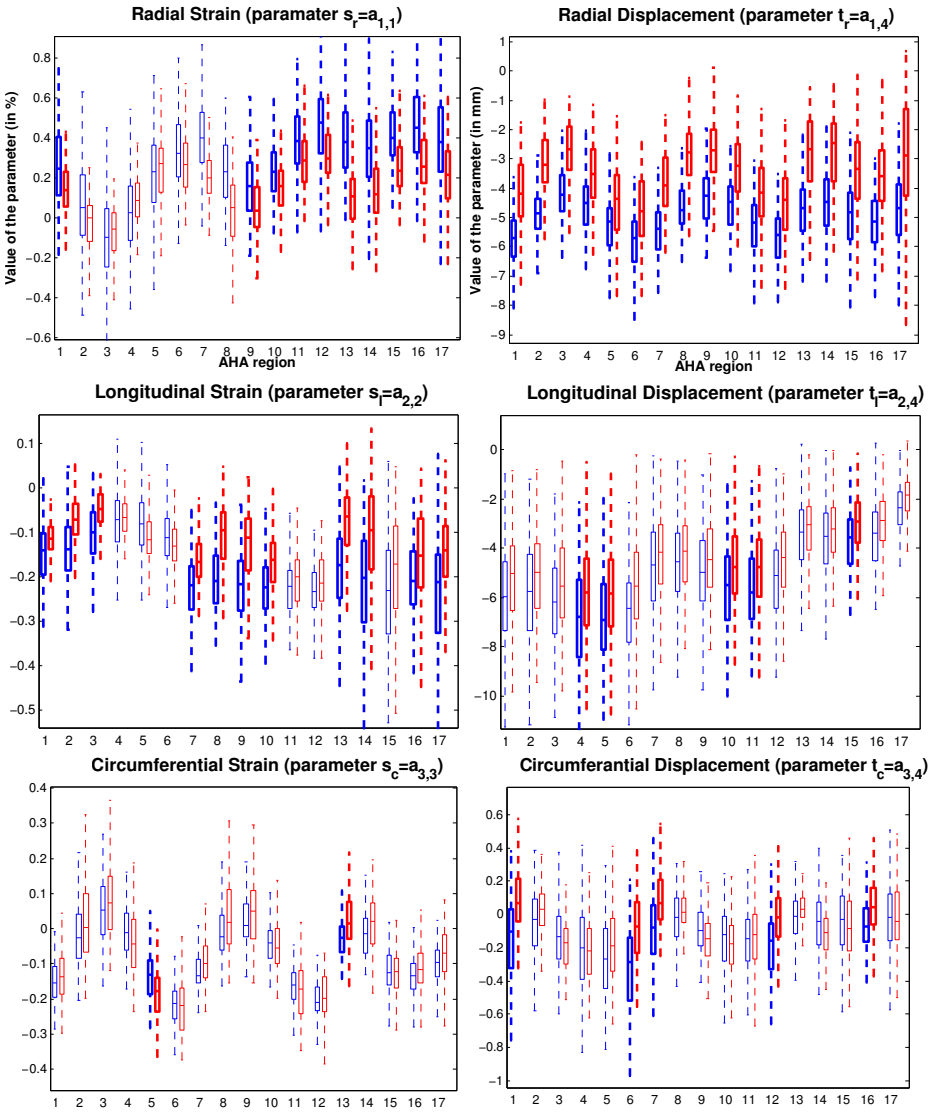


**Fig. 1.** Parameters of the polyaffine projection both for infarcted patients (red) and control subjects (blue). (Top row): radial parameters for both the diagonal parameters - representing strain - and the translation parameters - representing motion. (Middle row): longitudinal parameters. (Bottom row): circumferential parameters. In bold the most significant parameters ($p$-value $< 0.001$).

the AHA zones at ED and ES. These parameters correspond to the initial and final stages of the transformation from ED to ES, and therefore complement the above-described parameters. We define the thickness as the local distance

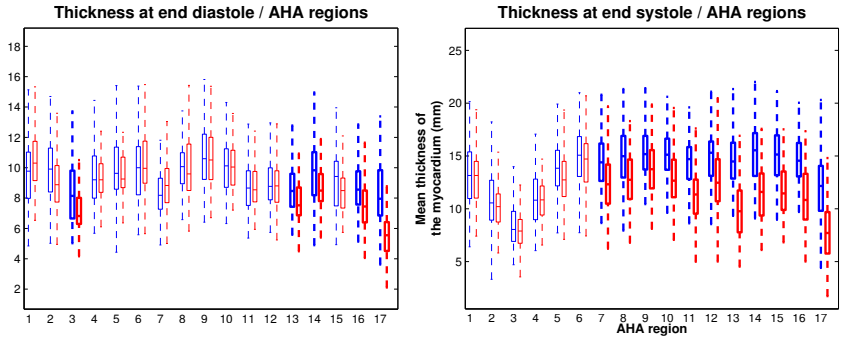


**Fig. 2.** Box-plots of the thickness of the myocardium wall per AHA region. In blue, the control set and in red the patients with infarcts. (Left): end-diastole. (Right): end-systole. In bold the most significant parameters ($p$-value $< 0.001$).

between endocardial points and their corresponding epicardial locations. These values are also averaged per AHA zone, and summarized in Fig. (2). Significant differences are observed in the thickness of the myocardium wall at end-systole in most of the regions, especially near the apex, for the diseased patients with respect to the control group. On the other side, thickness ED diastole is less discriminant between both groups. Other parameters related to shape were considered (such as the height of the heart at ED/ES and the diameter at the base at ED/ES) but no significant differences between both populations were seen and therefore we do not use them for classification.

## 3 Dimensionality reduction of the parameters and classification

In this section, we use both polyaffine and thickness parameters previously introduced in order to classify between healthy and infarcted subjects. We use the machine-learning toolbox Scikit-Learn [8] to test a collection of standard state-of-the-art algorithms on our dataset and compare their performance in predicting yet unseen data. The features that serve to feed the tested learned algorithms were considered in four different ways: either polyaffine or thickness parameters separately (sets # 1 and # 2), or concatenated without normalization (# 3) or with normalization so that they have a mean of 0 and a variance of 1.

### 3.1 Learnt Dimensionality Reduction

Complementary to the a-priori reduction of dimensionality imposed by the polyaffine model and the use of 17 AHA regions, we also evaluated the influence of a second dimensionality reduction of the data both with a Principal Component Analysis (PCA) and a Principal Least Square (PLS) decomposition [9] prior to the tested algorithm. PCA is designed to spread the data according to the main modes

| | | | STRAIN | | | TRANSLATION | | | THICKNESS | | |
|---|---|---|---|---|---|---|---|---|---|---|---|
| | | | RADIAL | LONG | CIRC | RADIAL | LONG | CIRC | END DIASTOLE | END SYSTOLE | SUM OVER ALL PARAMETERS |
| AHA REGIONS | BASE | 1 | 0.9% | 0.3% | 0.0% | 2.1% | 0.9% | 0.5% | 0.0% | 0.2% | 5% |
| | | 2 | 0.4% | 0.9% | 0.0% | 2.3% | 0.9% | 0.1% | 0.2% | 0.2% | 5% |
| | | 3 | 0.0% | 0.6% | 0.0% | 2.0% | 1.2% | 0.0% | 0.3% | 0.2% | 4% |
| | | 4 | 0.0% | 0.0% | 0.2% | 1.5% | 1.3% | 0.0% | 0.0% | 0.0% | 3% |
| | | 5 | 0.1% | 0.1% | 0.3% | 1.2% | 1.2% | 0.2% | 0.0% | 0.2% | 3% |
| | | 6 | 0.5% | 0.0% | 0.0% | 1.5% | 1.0% | 0.5% | 0.0% | 0.2% | 4% |
| | MIDDLE | 7 | 1.9% | 1.4% | 0.2% | 2.3% | 0.8% | 0.5% | 0.0% | 0.8% | 8% |
| | | 8 | 1.3% | 1.6% | 0.2% | 2.6% | 0.9% | 0.0% | 0.0% | 0.8% | 7% |
| | | 9 | 0.9% | 1.6% | 0.1% | 2.4% | 1.1% | 0.1% | 0.0% | 0.6% | 7% |
| | | 10 | 0.8% | 1.3% | 0.0% | 1.9% | 1.2% | 0.0% | 0.0% | 0.7% | 6% |
| | | 11 | 0.9% | 0.5% | 0.0% | 1.5% | 1.2% | 0.0% | 0.0% | 0.7% | 5% |
| | | 12 | 1.5% | 0.6% | 0.0% | 1.7% | 1.0% | 0.4% | 0.0% | 0.6% | 6% |
| | APICAL | 13 | 1.9% | 1.3% | 0.4% | 2.5% | 0.8% | 0.1% | 0.3% | 1.6% | 9% |
| | | 14 | 1.6% | 1.2% | 0.2% | 2.2% | 1.0% | 0.1% | 0.2% | 1.2% | 8% |
| | | 15 | 1.4% | 0.7% | 0.0% | 1.6% | 1.1% | 0.0% | 0.1% | 1.1% | 6% |
| | | 16 | 1.7% | 0.7% | 0.1% | 1.8% | 0.9% | 0.4% | 0.3% | 1.1% | 7% |
| | APEX | 17 | 1.2% | 1.1% | 0.4% | 1.5% | 1.0% | 0.0% | 0.6% | 1.1% | 7% |
| SUM OVER ALL REGIONS | | | 17.0% | 13.8% | 2.2% | 32.7% | 17.8% | 3.0% | 2.1% | 11.4% | |

**Fig. 3.** Loadings of the first PLS mode showing the contribution of each of the parameters and each of the AHA zone. In green the most important parameters and in red the less important.

of variability and is known to be a useful dimension reduction pre-processing to prevent over-fitting and improve the performance of some machine-learning algorithm. PLS looks at modes of the input variables that correlate the most with an output variable (in our case the pathology label 0 or 1). Therefore, in contrast with PCA, the modes also correlate with our classification. In particular, Fig 3 summarizes the loadings of the first mode of the PLS with respect to each parameter. Notably, this can be used to assess which of the parameters is the most important for the classification. The radial parameters are the most prevalent, whereas both the circumferential parameters and the thickness at ED provide very little contribution to the first mode and therefore the classification.

### 3.2 Classification

All algorithms were tested with 10-fold cross validation on the dataset made of 200 patients. Fig. 4 summarizes the results of the different algorithms. Combining both sets of parameters improves the performance of most of the algorithms showing that these sets give different kind of information about the data. We also see that PLS regression, by preprocessing the data and orienting the modes of the input variables upto the best correlation with the pathology labels, improves the performance of all machine learning algorithms especially for Decision Tree and Nearest Neighbors. With more than 95% of correct labeling, SVM-SVC algorithm used on the PLS reduction with 5 modes is the method that performs the best. It is interesting to see that increasing the number of PLS modes further

| | | Decision Tree | Random Forest | Logistic Regression | Nearest Neighbors | SVM Linear | SVM svc |
|---|---|---|---|---|---|---|---|
| | PolyAffine (PA) | 79% | 88% | 85% | 81% | 89% | 86% |
| | Thickness (TH) | 76% | 84% | 86% | 89% | 85% | 86% |
| | PA + TH | 79% | 91% | 89% | 90% | 90% | 92% |
| | Norm. PA + TH | 77% | 88% | 92% | 85% | 90% | 94% |
| PCA | 2 Modes | 84% | 87% | 90% | 89% | 87% | 89% |
| | 5 Modes | 84% | 87% | 90% | 87% | 88% | 93% |
| | 10 Modes | 84% | 89% | 90% | 87% | 88% | 93% |
| | All modes | 84% | 80% | 93% | 87% | 92% | 96% |
| PLS | 2 Modes | 91% | 93% | 94% | 94% | 93% | 94% |
| | 5 Modes | 91% | 96% | 96% | 97% | 95% | 97% |
| | 10 Modes | 91% | 97% | 96% | 94% | 95% | 96% |
| | All modes | 91% | 94% | 94% | 94% | 93% | 94% |

**Fig. 4.** Cross-validation results (10-fold) of the classification with respect to different state-of-the-art machine learning algorithms and different sets of input data. Combination of algorithms and parameters that have the best performance are shown in green whereas the worst are shown in red.

does not improve the classification. Our interpretation is that the subsequent modes of the PLS are not correlated to the classification and can therefore induce over-fitting of the data. We also tested the method with different cross-validation such as leave-one-out, 2-fold or 5-fold in order to see the robustness of the method with respect to the size of the training set and got similar performance.

## 4 Conclusion

In this paper, we evaluated the contribution of prior reduction of dimensionality to the classification of high-dimensional motion data. One of the assets of our work is an innovative methodology to project a motion on a reduced number of polyaffine parameters. We apply the methodology to classify a population and detect an infarct based on the segmentations at end-systole and end-diastole. Following the first dimensionality reduction given by the polyaffine parameters, we use traditional statistical reductions on our sets of parameters with PCA and PLS. Using 10-fold cross validation, we show that the resulting parameters have good predictive power with more than 95 % correct classification on 200 infarcted/control cases. We are also able to quantify the importance of each of the parameters in the classification. Notably, this provides insights into what is the main impact of an infarct both in terms of motion and shape.

*Ackowledgements* The authors acknowledge the partial funding by the EU FP7-funded project MD-Paedigree (Grant Agreement 600932)

## References

1. Konstam, M.A., Kramer, D.G., Patel, A.R., Maron, M.S., Udelson, J.E.: Left ventricular remodeling in heart failure. current concepts in clinical significance and assessment. JACC: Cardiovascular Imaging (2011)

2. Bijnens, B., Claus, P., Weidemann, F., Strotmann, J., Sutherland, G.: Investigating cardiac function using motion and deformation analysis in the setting of coronary artery disease. Circulation (2007)
3. Sudarshan, V., Acharya, U.R., Yin-Kwee Ng, E., Meng, C.S., Tan, R.S., Ghista, D.N.: Automated Identification of Infarcted Myocardium Tissue Characterisation Using Ultrasound Images: A Review. IEEE Reviews in Biomedical Engineering (2013)
4. Fonseca, C., Backhaus, M., Bluemke, D., Britten, R., Chung, J., Cowan, B., Dinov, I., Finn, J., Hunter, P., Kadish, A., Lee, D., Lima, J., Medrano-Gracia, P., Shivkumar, K., Suinesiaputra, A., Tao, W., Young, A.: The cardiac atlas project–an imaging database for computational modeling and statistical atlases of the heart. Bioinformatics **27**(5) (2011-08-15 00:00:00.0) 2288–95
5. Zhang, X., Ambale-Venkatesh, B., Bluemke, D., Cowan, B., Finn, J., Hundley, W., Kadish, A., Lee, D., Lima, J., Suinesiaputra, A., Young, A., Medrano-Gracia, P.: Orthogonal shape modes describing clinical indices of remodeling. In: Functional Imaging and Modeling of the Heart. (2015)
6. Arsigny, V., Commowick, O., Ayache, N., Pennec, X.: A fast and log-Euclidean polyaffine framework for locally linear registration. Journal of Mathematical Imaging and Vision (2009)
7. McLeod, K., Sermesant, M., Beerbaum, P., Pennec, X.: Spatio-temporal tensor decomposition of a polyaffine motion model for a better analysis of pathological left ventricular dynamics. IEEE Trans. Med. Imaging (2015)
8. Pedregosa, F., Varoquaux, G., Gramfort, A., Michel, V., Thirion, B., Grisel, O., Blondel, M., Prettenhofer, P., Weiss, R., Dubourg, V., Vanderplas, J., Passos, A., Cournapeau, D., Brucher, M., Perrot, M., Duchesnay, E.: Scikit-learn: Machine learning in Python. Journal of Machine Learning Research **12** (2011) 2825–2830
9. Rosipal, R., Krämer, N.: Overview and recent advances in partial least squares. In: Subspace, latent structure and feature selection. (2006)